



The top of the Olduvai Subchron in a high-resolution magnetostratigraphy from the West Turkana core WTK13, hominin sites and Paleolakes Drilling Project (HSPDP)

Mark J. Sier^{a, b, c, *}, Cor G. Langereis^a, Guillaume Dupont-Nivet^{d, j}, Craig S. Feibel^e, Josephine C.A. Joordens^{c, f}, Jeroen H.J.L. van der Lubbe^f, Catherine C. Beck^g, Daniel Olago^h, Andrew Cohenⁱ, WTK Science team members¹

^a Faculty of Geosciences, Utrecht University, P.O. Box 80021, 3508 TA, Utrecht, The Netherlands

^b Oxford University, Department of Earth Sciences, South Parks Road, OX1 3AN, Oxford, United Kingdom

^c Faculty of Archaeology, Leiden University, P.O. Box 9515, 2300 RA, Leiden, The Netherlands

^d Géosciences Rennes UMR-CNRS 6118, Rennes, France

^e Department of Earth and Planetary Sciences, Rutgers University, Piscataway, NJ 08854, USA

^f Faculty of Sciences, VU University Amsterdam, De Boelelaan 1085, 1081 HV, Amsterdam, The Netherlands

^g Department of Geosciences, Hamilton College, Clinton, NY 13323, USA

^h Department of Geology, University of Nairobi, Nairobi, Kenya

ⁱ Department of Geosciences, University of Arizona, Tucson, AZ 85721, USA

^j Institute of Earth and Environmental Science, Potsdam University, Karl-Liebknecht-Str. 24-25, 14476 Potsdam-Golm, Germany

ARTICLE INFO

Article history:

Received 26 December 2016

Received in revised form

29 May 2017

Accepted 22 August 2017

Available online 26 August 2017

Keywords:

Paleolake Lorenyang

Magnetostratigraphy

Olduvai Subchron

Vrica Subchron

Drill-core reorientation

ICDP

Paleoclimate

Hominin evolution

ABSTRACT

One of the major challenges in understanding the evolution of our own species is identifying the role climate change has played in the evolution of hominin species. To clarify the influence of climate, we need long and continuous high-resolution paleoclimate records, preferably obtained from hominin-bearing sediments, that are well-dated by tephro- and magnetostratigraphy and other methods. This is hindered, however, by the fact that fossil-bearing outcrop sediments are often discontinuous, and subject to weathering, which may lead to oxidation and remagnetization. To obtain fresh, unweathered sediments, the Hominin Sites and Paleolakes Drilling Project (HSPDP) collected a ~216-meter core (WTK13) in 2013 from Early Pleistocene Paleolake Lorenyang deposits in the western Turkana Basin (Kenya). Here, we present the magnetostratigraphy of the WTK13 core, providing a first age model for upcoming HSPDP paleoclimate and paleoenvironmental studies on the core sediments. Rock magnetic analyses reveal the presence of iron sulfides carrying the remanent magnetizations. To recover polarity orientation from the near-equatorial WTK13 core drilled at 5°N, we developed and successfully applied two independent drill-core reorientation methods taking advantage of (1) the sedimentary fabric as expressed in the Anisotropy of Magnetic Susceptibility (AMS) and (2) the occurrence of a viscous component oriented in the present day field. The reoriented directions reveal a normal to reversed polarity reversal identified as the top of the Olduvai Subchron. From this excellent record, we find no evidence for the 'Vrica Subchron' previously reported in the area. We suggest that outcrop-based interpretations supporting the presence of the Vrica Subchron have been affected by the oxidation of iron sulfides initially present in the sediments – as evident in the core record – and by subsequent remagnetization. We discuss the implications of the observed geomagnetic record for human evolution studies.

Crown Copyright © 2017 Published by Elsevier B.V. All rights reserved.

1. Introduction

Many of the evolutionary changes in our human lineage are thought to have been strongly influenced by changes in climate and environment (e.g. Behrensmeyer, 2006; deMenocal, 2011; Joordens

* Corresponding author. Oxford University, Department of Earth Sciences, South Parks Road, OX1 3AN, Oxford, United Kingdom.

E-mail address: marksier@gmail.com (M.J. Sier).

¹ listed at <https://hspdp.asu.edu>.

et al., 2011; Levin, 2015; Potts, 2013; Vrba, 1995). To test hypotheses concerning these driving forces, it is essential to place hominin fossils in a precise chronological and climatic-environmental framework (Behrensmeyer, 2006; Campisano et al., 2017). The Hominin Sites and Paleolakes Drilling Project (HSPDP) is a project of the International Continental Drilling Program (ICDP) and aims at reconstructing climatic changes and associated environmental conditions during hominin evolution (Campisano et al., 2017; Cohen et al., 2016). To this end, cores were drilled in ancient lake beds in the East African Rift System (Ethiopia and Kenya) targeting sediments from some of the most important hominin sites in the world, covering the last 3.5 Ma. Here, we report on a detailed magnetostratigraphic record in sediments from the core WTK13 drilled by HSPDP in 2013 adjacent to the Kaitio laga (dry river bed), West Turkana, Kenya (Fig. 1). The sedimentary sequence at this location archives human evolutionary and climatic events between ~2.0 and 1.35 Ma (Brown et al., 2006; Cohen et al., 2016; Feibel, 2011). This is a key period in human evolution because from ~2.0 Ma onwards, several early *Homo* species, together with *Paranthropus boisei*, roamed the landscape around paleolake Lorenyang in the Turkana Basin, and at ~1.9 Ma *Homo erectus/ergaster* made its first appearance there (Joordens et al., 2013, 2011; Leakey et al., 2012; Spoor et al., 2015). The *Homo erectus/ergaster* fossil “Turkana Boy” (or Nariokotome Boy), the most complete skeleton of its species ever found and dated to around 1.6 Ma, was recovered at Nariokotome (Harris et al., 1985) close to the drill site. Moreover, the earliest Acheulian tools with an age of around 1.76 Ma were recovered at Kokiselei (Lepre et al., 2011) just to the southwest of the Kaitio laga (Fig. 1C), emphasizing the significance of WTK13 for hominin evolution and archaeological studies.

Magnetostratigraphy has been a critical tool for the development of age models in many ICDP and International Ocean Discovery Program (IODP) projects (e.g. Channell, 2017; Channell et al., 2016; Cohen et al., 2016), and has also proven to be useful in numerous prior outcrop-based stratigraphic studies of hominin sites (e.g. Dupont-Nivet et al., 2008; Lepre and Kent, 2010; Lepre et al., 2011; Joordens et al., 2013, 2011; Maddy et al., 2015; Parés et al., 2013). Drilling provides a unique opportunity to circumvent problems typically encountered in outcrops. It allows obtaining long continuous stratigraphic intervals not biased by major faults, folds, or diachronous lateral discontinuities in the stratigraphic record, which can be readily sampled at high-resolution. Most importantly, drilling enables the recovery of sediments that are more likely to have preserved a primary magnetization because they have been less exposed to post-depositional weathering. This is particularly critical for organic-rich lake deposits that are easily oxidized and thus often remagnetized, which hinders a straightforward identification of the paleomagnetic record.

In drilling projects, deriving the polarity of the ancient magnetic field relies on the orientation of the paleomagnetic inclination: down (up) for normal (reversed) polarity for sediments deposited at northern latitudes. For sites at low latitudes, however, the inclination cannot be used because it is close to zero for both normal and reversed polarities. For sites at these latitudes one needs to recover the paleomagnetic declination: North (South) for normal (reversed) polarity. Unfortunately, due to the rotation of core segments during standard drilling and core recovery, the declination is usually randomly re-distributed. To overcome this problem, several sampling techniques can be applied such as inclined drilling and/or azimuthal orientation of core segments using various orientation devices (Cohen et al., 2016). In addition, specific paleomagnetic data processing techniques can help to circumvent the problem and recover paleomagnetic declinations (e.g. Hailwood and Ding, 1995).

Here we present the magnetostratigraphy of the 216-meter long

core with a core recovery of 94.1% (WTK13, stored at the LacCore Facilities of the University of Minnesota) that was drilled in 2013 at an angle of 10° in slightly tilted (~5°) deposits of paleolake Lorenyang in the western Turkana Basin (Fig. 1) as part of the HSPDP project (Cohen et al., 2016). We report a set of custom paleomagnetic data processing techniques that successfully enabled us to overcome the challenges inherent to interpreting paleomagnetic data from cores drilled at low latitudes. This allows us to provide the first high-resolution magnetostratigraphy of core WTK13. We also discuss the implications of the observed structure for the upper part of the Olduvai Subchron and its implications for remagnetization of outcrop sediments.

2. Background

2.1. Geological setting

The Turkana Basin in southern Ethiopia and northern Kenya (Fig. 1A) lies within the East African Rift System (McDougall et al., 2012). Accumulation of sediments started in the Turkana Basin at ~4.2 Ma (Brown and McDougall, 2011; McDougall and Brown, 2008) and continues to this day. Since at least ~4.2 Ma, a major fluvial system (Omo River) drains the Ethiopian Highlands and brings water into the Turkana Basin. During this time period a meandering river system alternated with several lake phases in the Turkana Basin, including a long lived (from ~2 to 1.5 Ma) basin-wide lake system known as Paleolake Lorenyang (Brown and Feibel, 1991; Feibel, 2011; Feibel et al., 1991).

Strata with ages ranging from 4.2 to 1.2 Ma are referred to as the Omo Group (Brown et al., 2006; de Heinzelin, 1983), which consists of the Nachukui Formation exposed in the West Turkana region (Harris et al., 1988), the Koobi Fora Formation in East Turkana (Brown and Feibel, 1986) and the Shungura Formation in the lower Omo River Valley in the north of the basin (de Heinzelin and Haesaerts, 1983, Fig. 1B, D). Correlation between the different regions, and even within the same region, is not straightforward as a result of lateral variability in depositional environments, but is aided by correlating regional tephra and the recognition of well-dated paleomagnetic reversals (Feibel, 2011; McDougall et al., 2012). The HSPDP West Turkana core drilling recovered sediments deposited in Paleolake Lorenyang represented by the relatively expanded Natoo Member, Kaitio Member and part of the Kalochoro Member of the Nachukui Formation (Harris et al., 1988). The aim was to reach the well-dated Chari Tuff (1.38 ± 0.03 Ma) and KBS Tuff (1.87 ± 0.02 Ma) (McDougall and Brown, 2006), which are important interbasinal marker beds (Fig. 1D). In contrast to oceanic environments with low, yet very constant sediment accumulation rates, continental environments such as the Paleolake Lorenyang depositional system are characterized by a more dynamic and stochastic nature of sediment accumulation. They include sedimentological features such as prograding sequences, migrating sandstone bars, scouring surfaces, and frequent sedimentological changes. This typically results in highly variable accumulation rates in the order of 10–100 cm/kyr (Feibel et al., 2016, 2009; Joordens et al., 2013, 2011) and may entail the occurrence of short hiatuses in the order of several thousand years. These characteristic depositional features of continental cores will be taken into account in our interpretation of the WTK13 core magnetostratigraphy. The interval sampled in the WTK13 core is roughly estimated to cover roughly 1.9 to 1.4 Ma based on outcrop correlations (Cohen et al., 2016; Harris et al., 1988).

2.2. Previous chronostratigraphic studies in the Turkana Basin

The Plio-Pleistocene fossil and artefact-rich sediments of the

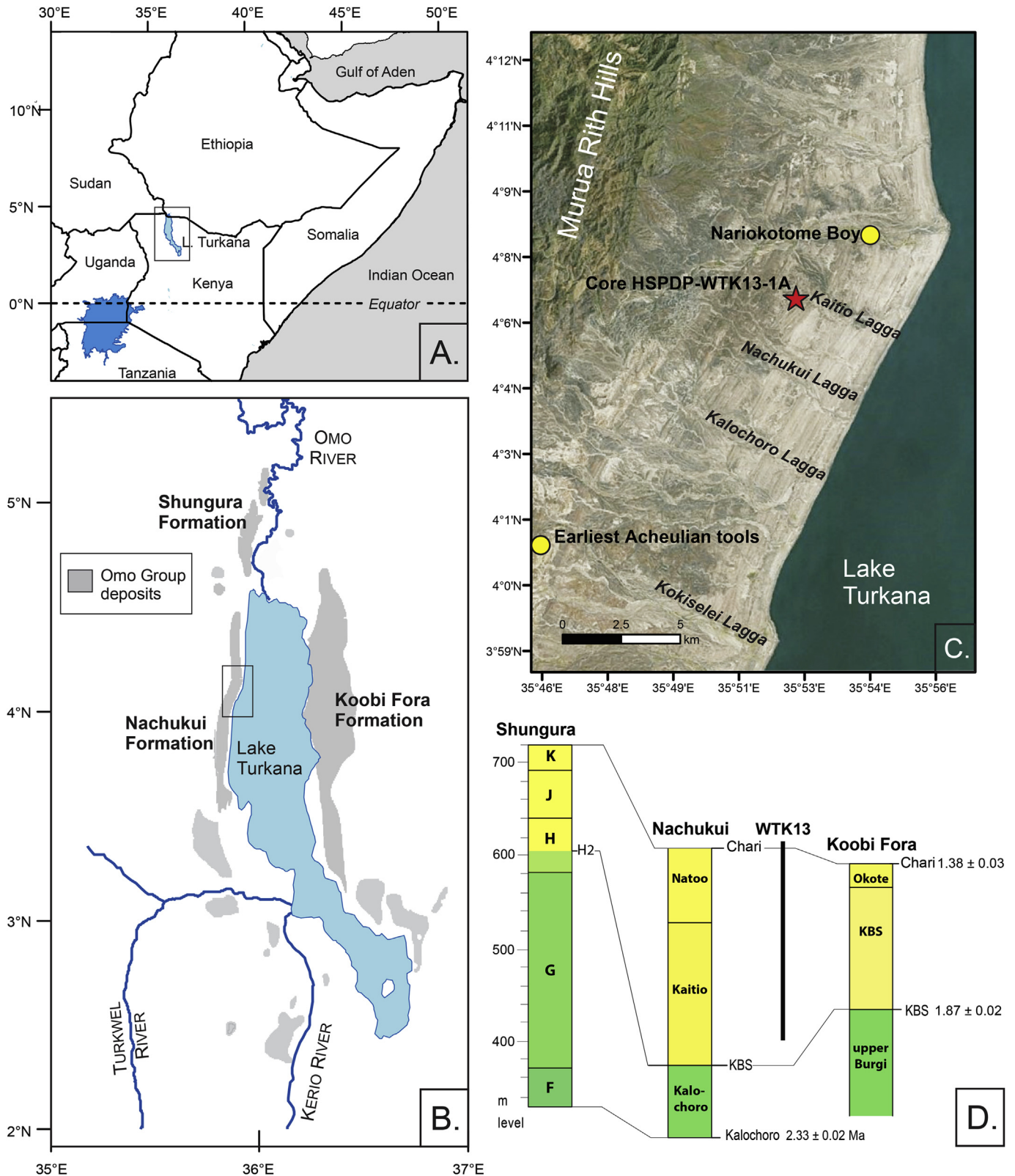


Fig. 1. a. Map of NE Africa. b. Map of the Turkana Basin with Omo Group deposits indicated in grey and the geographic location of the Shungura, Nachukui, and Koobi Fora Formations. c. Detailed Google Earth map of the western Turkana Basin. Red star: location of the WTK13 core (lat: 4.1097, long: 35.8718; Cohen et al., 2016). Yellow circle: find location of the *Homo erectus* skeleton Nariokotome Boy (Harris et al., 1985) and of the earliest Acheulian tools (Lepre et al., 2011). d. Composite stratigraphy of the Shungura, Nachukui and Koobi Fora Formation sequences between the Kalocho Tuff and the Chari Tuff (adapted from McDougall et al., 2012). We indicated the approximate span in the Nachukui Formation of core WTK13. (For interpretation of the references to colour in this figure legend, the reader is referred to the web version of this article.)

Turkana Basin make the region an important target for dating studies (Feibel, 2011; McDougall et al., 2012). Early work on the magnetostratigraphy of the Koobi Fora Formation on the east side of Lake Turkana was done by Brock and Isaac (1974), Hillhouse et al. (1977) and Brown et al. (1978). More recent paleomagnetic studies were carried out by Kidane et al. (2014, 2007), Lepre et al. (2011), Joordens et al. (2011, 2013) and Lepre and Kent (2015, 2010). A large number of tuffs and pumice layers, including the Chari and KBS Tuffs, have been dated and correlated within the Turkana Basin and beyond (McDougall et al., 2012 and references therein) providing a consistent and robust geochronological framework for interpretation of paleomagnetic results from the Omo Group deposits (Fig. 1D).

In the top of the Olduvai Subchron dated to 1.778 ± 0.003 Ma (Hilgen et al., 2012), an interval of reversed polarity has been inconsistently observed, creating an extra but short normal Subchron, the so called 'Vrica Subchron' (Zijderveld et al., 1991). The interval of reversed polarity has been argued by Roberts et al. (2010) to be the result of postdepositional remagnetization through formation of late diagenetic greigite at the type locality, based on observations from a drill core at Vrica, Italy. Several studies predating the definition of the Vrica Subchron found mixed polarities near the top of the Olduvai in the Turkana Basin (Brock and Isaac, 1974; Hillhouse et al., 1977), while some recent studies in the basin specifically argue for the existence of the Vrica Subchron (Lepre and Kent, 2015, 2010; Lepre et al., 2011). Since the top of the Olduvai Subchron is an important time anchor in hominin evolution and archaeology studies, a critical evaluation of the Vrica Subchron as a real geomagnetic feature is called for, and is developed in detail below in the discussion of our results.

3. Methods

3.1. The WTK13 core

The 216 m long WTK13 core is curated at the US National Lacustrine Core Facility (LacCore) of the University of Minnesota (USA). The technical background on the drilling of the core, and a first lithostratigraphy plus core color stratigraphy is provided in Cohen et al. (2016). These stratigraphies (Fig. 2a and b) show that the lower part of the core below ca. 60 meter below surface (mbs) consists of dark greenish lacustrine fine mudstones, whereas the top of the core is dominated by brownish fluvio-deltaic mudstones to sandstones (Feibel et al., 2016). Full lithostratigraphic descriptions of the WTK13 core sediments with depositional environment interpretations will be provided in a later publication within the HSPDP West Turkana collaboration.

3.2. Sampling the WTK13 core

At the LacCore facility, a total of about 700 samples at 662 levels were taken from the 216 metres of the WTK13 core with an average spatial resolution of ~32 cm. All encountered lithologies were sampled, unless the sediment was badly broken up due to the core drilling process. Occasional "disking" of the core was observed indicating that (parts of) core segments had rotated with respect to adjacent intervals during drilling.

All samples were oriented and logged with respect to the top of the core segment. The sample position within each core segment was measured with <0.5 cm precision. Several methods of sampling have been applied directly after splitting of the core. When possible, samples were taken with an (electrical) drill press equipped with a water-cooled diamond coated 2.5 cm diameter drill bit. Softer levels not drillable were sampled by gently pushing cylindrical cups into the sediment. We used two types of cups

depending on the type of experiments to be done. Samples for alternating field (AF) demagnetization were collected with perspex containers, whereas custom-made quartz glass containers were used to take samples for thermal (TH) demagnetization. Both sample containers have standard paleomagnetic sampling dimensions (25 mm diameter, 22 mm length). If the sediment was too fragile, or broke during application of the methods mentioned above, small hand samples were taken or the level was skipped. After labelling the samples, they were wrapped in airtight cellophane and stored at temperatures below 5° Celsius.

3.3. Rock magnetism

To assess the magnetic mineralogies of the sediments and their behavior upon heating, thermomagnetic curves were measured in air on a modified horizontal translation-type Curie balance with a sensitivity of around $5 \times 10^{-9} \text{ Am}^2$ (Mullender et al., 1993) at the Paleomagnetic Laboratory Fort Hoofddijk, Utrecht University (The Netherlands). This was done on three samples that were taken from lacustrine claystones at different depths in the core: sample 24Q-2-139 (70.57 mbs), sample 43Q-2-24 (117.99 mbs), and sample 72Q-3-42 (183.27 mbs). The samples were powdered by hand with a mortar, and weights (ranging between 4 and 8 mg) were accurately determined. The powder was put in a small container on a quartz rod, and the container was closed with quartz wool. The magnetic field was cycled between a minimum of 100 mT and a maximum of 300 mT. Heating and cooling cycles (with rates of 6° and 10 °C/min) were run using cycles 20–300, 200–400, 300–700 °C.

Hysteresis parameters give further information concerning domain state - and hence on paleomagnetic stability - of the relevant magnetic minerals in rocks. A total of 96 samples were measured for this parameter (Supplementary Table 1). For the measurements of hysteresis curves, a vibrating sample magnetometer (VSM, MicroMag Model 3900; Princeton Measurements) was used. The hysteresis curves were corrected for the paramagnetic contribution and the relevant hysteresis parameters (M_{sr} , M_s , H_{cr} , H_c) were determined. Their ratios M_{sr}/M_s , H_{cr}/H_c were then plotted in a Day plot (Day et al., 1977). We follow the approach of Dunlop (2002a,b) to interpret the results in terms of (mixtures of) superparamagnetic (SP), single domain (SD), pseudo single domain (PSD) and multi domain (MD). As a rule, SP magnetic grains are too small to carry a remanent magnetization but they contribute to hysteresis parameters. A large portion of SP grains means very fine-grained magnetic grains, and is often concurrent with fine-grained sediment. Alternatively, SP grains may be produced *in situ* by (postdepositional) diagenetic processes, e.g. because of paleosol formation.

3.4. Demagnetization and ChRM directions

Stepwise progressive Thermal (TH) demagnetization of the natural remanent magnetization (NRM) was done for 284 samples up to a maximum of 600° Celsius (with a few samples to 680 °C), in 16 temperature steps using an ASC thermal demagnetizer (residual field < 20 nT) at the Centro Nacional de Investigación sobre la Evolución Humana (CENIEH) in Burgos (Spain). After each step the remaining NRM was measured with a 2G DC-SQUID (type SRM 755) cryogenic magnetometer. NRM intensities were typically several orders of magnitude higher than the instrument sensitivity ($\sim 3 \times 10^{-12} \text{ Am}^2$). During the demagnetization process, the specimens stayed in a shielded environment.

Stepwise progressive Alternating Field (AF) demagnetization was done for 86 samples up to a maximum of 100 mT, in 18 alternating field steps using the integrated AF demagnetizer of the DC-SQUID magnetometer. The demagnetization results were

Core HSPDP-WTK13

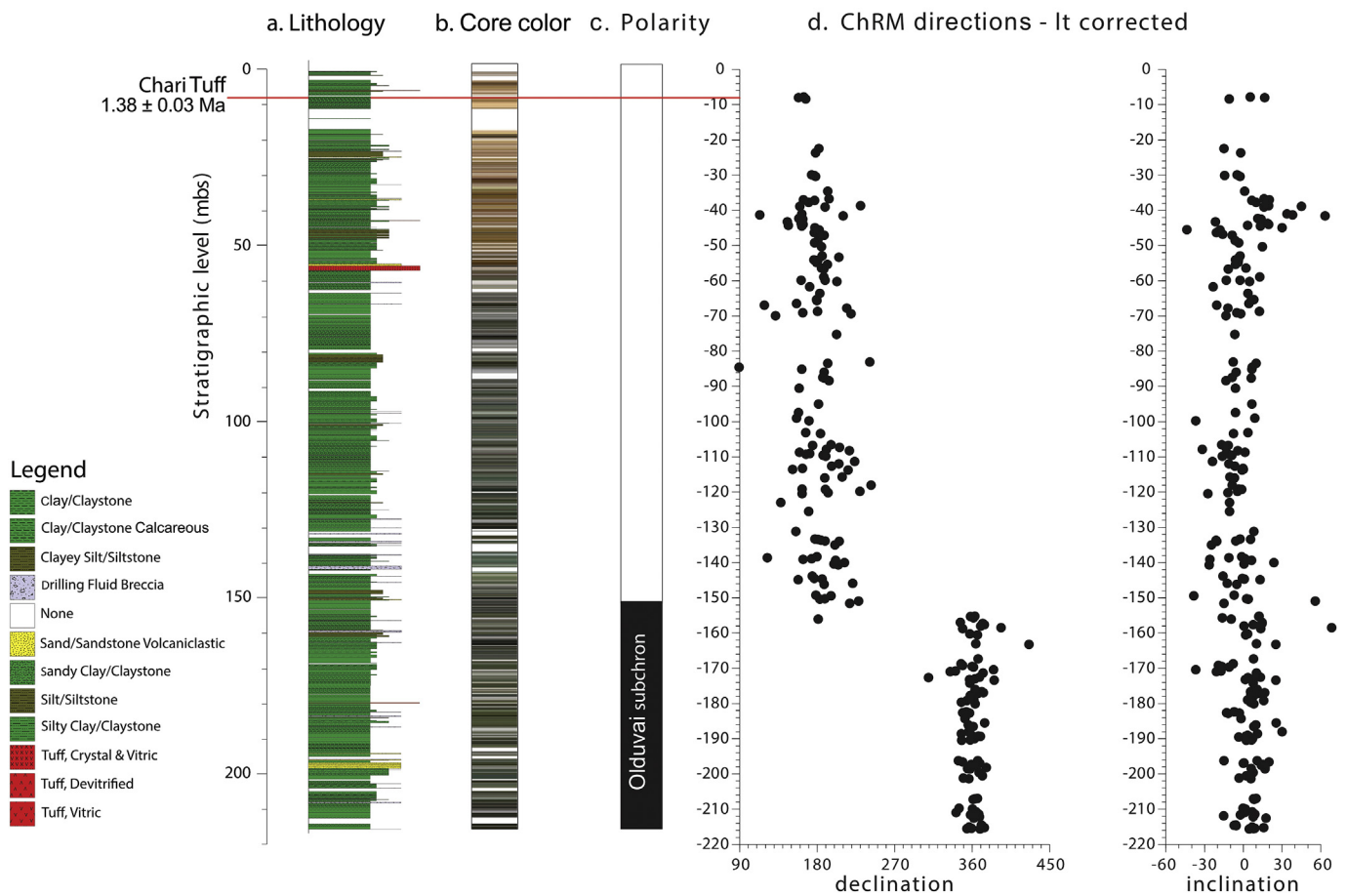


Fig. 2. Lithostratigraphic, core color and magnetostratigraphic results of the WTK13 core. a. Lithologic log rendered in PSICAT® with legend; missing core intervals are shown in white (Cohen et al., 2016). b. Core color stratigraphy from XYZ spectrophotometric imaging data, adjusted in Photoshop® using Image Adjustment Levels to maximize color range (Cohen et al., 2016); c. Magnetic polarity with white/black being reversed/normal paleomagnetic directions. d. ChRM directions WTK13 corrected for low temperature (LT) paleomagnetic directions, used to reorient the interpreted ChRM direction. See text for further explanation. (For interpretation of the references to colour in this figure legend, the reader is referred to the web version of this article.)

interpreted in terms of components to identify the ChRM directions using Paleomagnetism.org, an online multi-platform open source environment for paleomagnetic data analysis (Koymans et al., 2016). A minimum of four consecutive steps was considered to define directions (See [Supplementary Table II](#)). The environment uses a suite of techniques to statistically interpret the results (Deenen et al., 2011; Fisher, 1953; Kirschvink, 1980; Tauxe et al., 2010; Zijdeveld, 1967).

3.5. Anisotropy of magnetic susceptibility (AMS)

The Anisotropy of magnetic susceptibility (AMS) was measured for 325 samples (See [Supplementary Table III](#)) with an Agico MFK1-FA Kappa Bridge. The AMS is a petrofabric tool useful for determining the preferred orientation of magnetically dominant minerals. It is commonly used to determine the sedimentary and/or tectonic fabric of rocks (e.g. Hrouda, 1982). The AMS is usually geometrically described by an ellipsoid, whose axes are the minimum (k_{\min}), intermediate (k_{int}), and maximum (k_{\max}) axis of susceptibility (Hrouda, 1982). During deposition, sedimentary rocks acquire a so-called 'sedimentary fabric' characterized by the k_{\max} and k_{int} axes dispersed within the horizontal plane (sub) parallel to the bedding plane, whereas the k_{\min} axis is perpendicular to the

bedding plane because of compaction. A sedimentary fabric can be partially overprinted by a 'tectonic fabric' during incipient deformation. The result of the latter process is the development of a magnetic lineation (L) whereby k_{\max} axes align parallel to the minimum axis of stress (extension) or, equivalently, to the maximum axis of stress (compression). An AMS lineation can also be produced by laminar flow during deposition in very dynamic environments such as turbidites (Hrouda, 1982).

3.6. Reorientation of ChRM directions and magnetostratigraphy

As explained in the introduction, the low latitude of the WTK13 core locality is a major challenge for recovering polarity orientations. To overcome this challenge, the WTK13 core was drilled at an angle of 10° from vertical, in a western direction, to aid in determining polarity (Cohen et al., 2016). The 10° of the coring added to the local 5° westward dip of the bedding plane, provided an apparent total dip of 15° for the sediment layers in the core. This angle, however, proved to be insufficient to discriminate between normal and reversed polarity direction using the observed paleomagnetic inclination as shown in the results below (Fig. 2, [Supplementary Table II](#)). We therefore applied two independent methods to reorient core segments using: (1) the bedding dip

orientation preserved in the sedimentary fabric expressed by the AMS tensor principal directions (see details below and in Fig. 7), and (2) the occurrence of viscous present-day magnetic overprints indicating a northward direction (Fuller, 1969). The success of such methods depends strongly on sediment properties (fresh or weathered, transport currents, compaction, diagenesis, etc.) and their tectonic deformation that was assessed carefully.

4. Results

4.1. Rock magnetic results

As expected from the general organic-rich nature of the WTK13 core sediments and the observation of pyrite (FeS_2) and greigite (Fe_3S_4) upon splitting the lower part of the WTK13 core, the Curie balance curves suggest that iron sulfides constitute an important part of the magnetic minerals present. The heating and cooling curves show a loss of magnetization already below 300 °C in sample 24Q-2-139 (stratigraphic level 70.57 mbs; Fig. 3a). The presence of pyrite is clear from the increase in magnetization above 420 °C when fine-grained magnetite is formed (Passier et al., 2001). Also the Curie curve of sample 72Q-3-42 (183.27 mbs; Fig. 3b) shows the demagnetization of greigite and corresponding loss of remanence between 200 °C and 400 °C. However, in this sample there is also evidence for magnetite or even some maghemite, but here the presence of pyrite is not indicated by the results. Also in sample 43Q-2-24 (117.99 mbs; Fig. 3c) the rapid loss of remanence at an already low temperature (150–200 °C) suggests the presence of greigite. Considering the low temperature at which the remanence rapidly decays, this could indicate that the greigite is of biogenic origin and very fine-grained (e.g. Roberts et al., 2010).

Hysteresis curves (Fig. 4, Supplementary Table I) also suggest evidence for mostly greigite-like minerals and occasionally magnetite. There are no indications for high-coercive minerals, or a mixture of low and high coercive minerals, since there are no wasp-waisted or pot-bellied shapes (Tauxe et al., 1996). Saturation is typically reached at 150–200 mT which corresponds well with magnetite but also with greigite (e.g. Roberts et al., 2011; Vasiliev et al., 2007). Typical values for H_c range from 5 to 20 mT, whereas H_{cr} values range between 25 and 60 mT. These H_{cr} values usually correspond to a wide range of magnetic minerals, such as (titano) magnetite, fine-grained maghemite, greigite and pyrrhotite (e.g. Özdemir and Dunlop, 1997; Peters and Dekkers, 2003) in different grain-size ranges. However, this range of H_{cr} values excludes the presence of hematite and goethite. A Day plot of the ratios M_{sr}/M_s and H_{cr}/H_c shows that most values plot in the PSD box, but the distribution does not follow typical SD + MD/PSD behavior of magnetite, according to the theoretical mixing curves of Dunlop (2002a, 2002b) (Fig. 4). This may suggest the presence of a relative significant contribution of SP magnetite, however, the Curie balance results above suggest a more important iron sulfide contribution. In fact, the distribution of the ratios in the Day plot corresponds remarkably well with the greigite distribution of Roberts et al. (2011) for a range of grain-sizes and from various environments.

4.2. Demagnetization results

Of 662 levels sampled, 370 specimens were demagnetized thermally and/or by alternating field (Supplementary Table II). The Zijderveld diagrams (Fig. 5) indicate a low temperature (LT)/low coercive (LC) component up to 200–250 °C/25–30 mT. After removal of the LT/LC component, a high temperature (HT) or high-coercive (HC) magnetic component, which we considered to represent a characteristic remanent magnetization (ChRM),

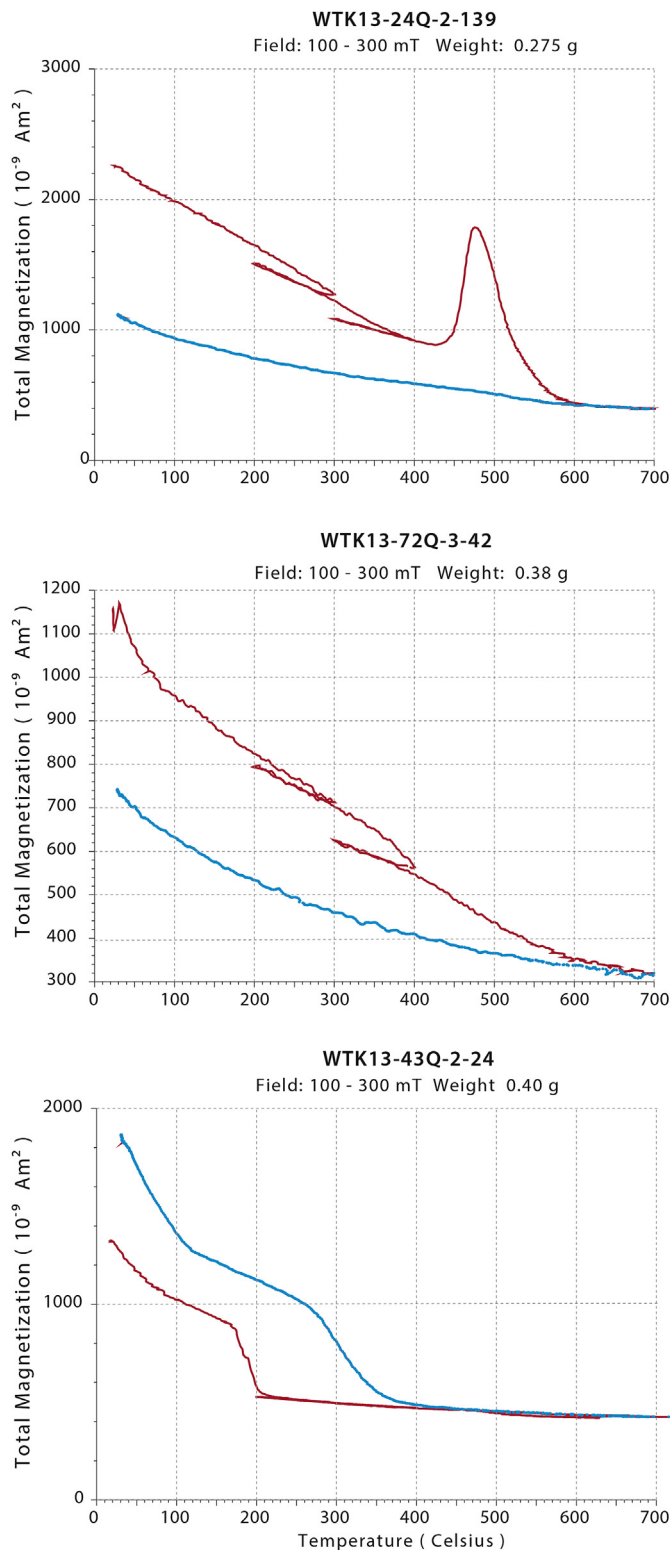


Fig. 3. Thermomagnetic experiments showing typical high-field magnetic moment upon heating and subsequent cooling in successive temperature ranges measured on a Curie balance, with heating curve in red and cooling curve in blue. Samples WTK13-1A-24Q-2-139 (70.57 mbs), WTK13-1A-72Q-3-42 (183.27 mbs) and WTK13-1A-43Q-2-24 (117.99 mbs). (For interpretation of the references to colour in this figure legend, the reader is referred to the web version of this article.)

demagnetized linearly. Typical ChRM directions were thus calculated using a minimum of four consecutive steps between 30 and

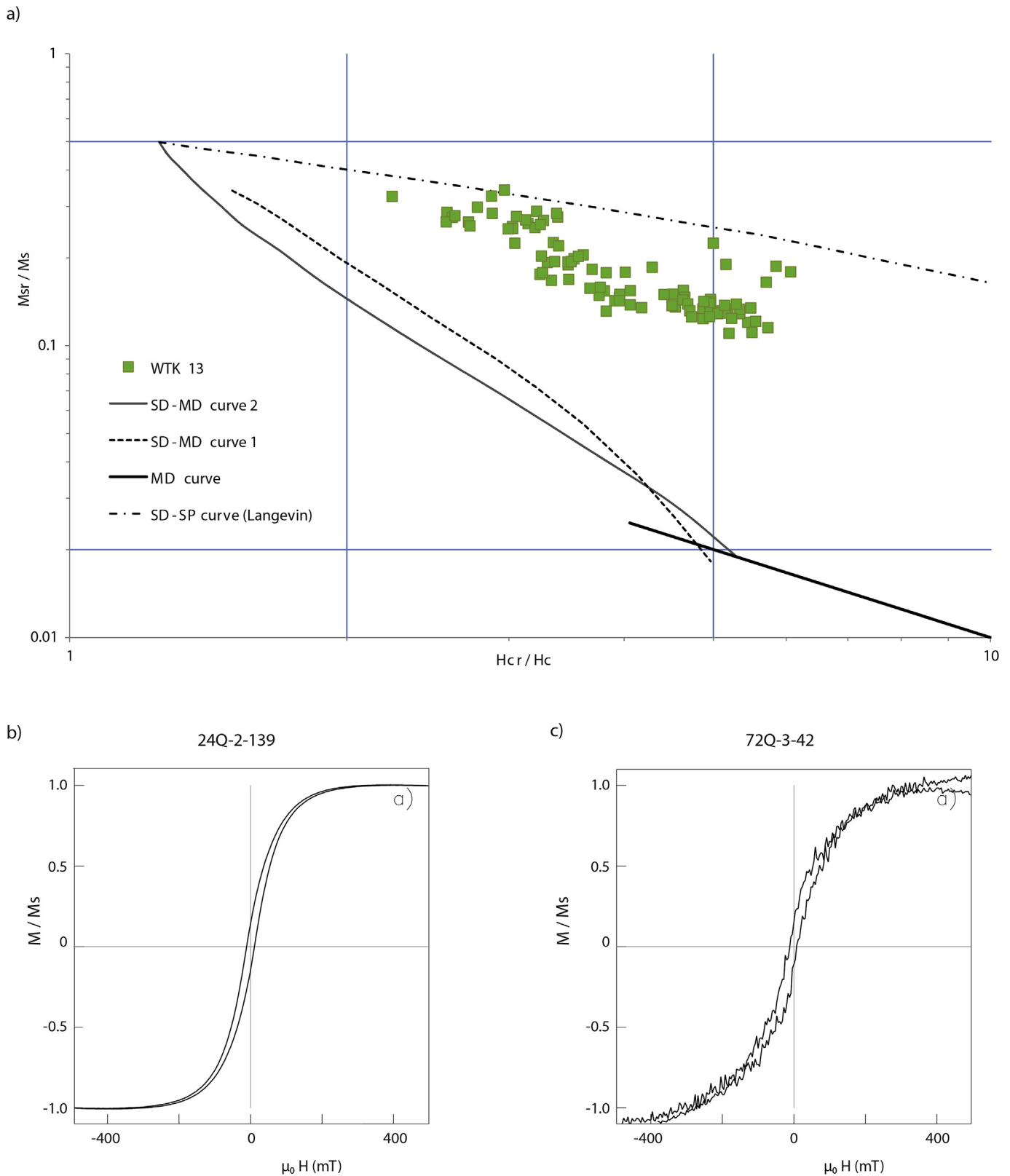


Fig. 4. a. Day plot of M_{sr}/M_s and H_{cr}/H_c ratios. The solid and dashed lines represent mixing curves of Dunlop (2002a,b), with SD = single domain, SP = superparamagnetic, and MD = multidomain. The data points (green squares) are from WTK13 core. SD range: M_{sr}/M_s 0.5 to 1 H_{cr}/H_c 1 to 2, PSD range: M_{sr}/M_s 0.5 and 0.04 H_{cr}/H_c 2 and 5, MD range: M_{sr}/M_s 0 to 0.04 H_{cr}/H_c bigger than 5. b. and c. hysteresis curves of samples WTK13-1A-24Q-2-139 (70.57 mbs) and WTK13-1A-72Q-3-42 (183.27 mbs). (For interpretation of the references to colour in this figure legend, the reader is referred to the web version of this article.)

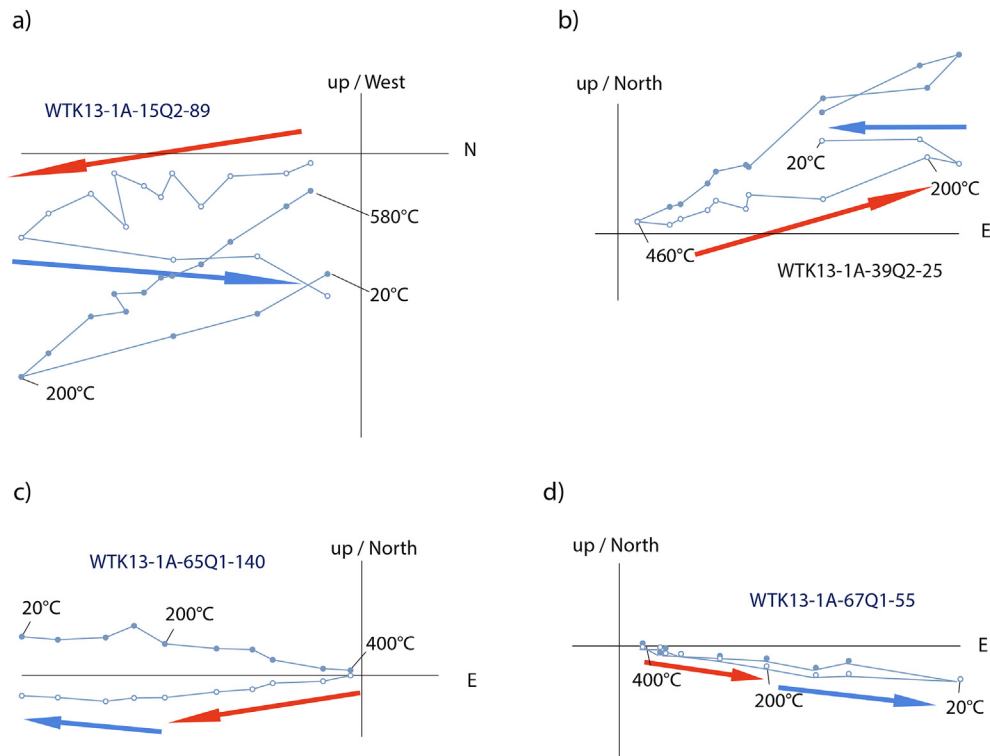


Fig. 5. Typical Zijdeveld (1967) diagram examples of two samples (a, b) with reversed ChRM (red arrow) after reorientation of the low temperature overprint to normal directions (blue arrow) and two examples of normal ChRM after reorientation (c, d). Closed/open circles denote projection on a horizontal/vertical plane. (For interpretation of the references to colour in this figure legend, the reader is referred to the web version of this article.)

80 mT and between 200 °C and 400 °C, or above if linear decay extended to higher temperatures. In the lower, more organic rich part of the core, usually linear decay extended up to around 400–430 °C (Fig. 5c and d). At higher temperatures, spurious magnetization behavior yielded erratic demagnetization paths often with increasing intensities. These behaviors are likely related to transformation of iron sulfides such as pyrite and greigite into fine-grained magnetite. In the upper part of the core, however, linear decay extended to higher temperatures, generally up to 580 °C (Fig. 5a). This temperature points to magnetite-like minerals as the main remanence carrier. Occasionally, linear decay extended up to 620 °C which points to a potential small contribution of maghemite. The plotted ChRM directions of the WTK core, without any correction for azimuthal orientation, show a scattered shotgun pattern in which no coherent polarity zonation can be recognized (see Supplementary Fig. 1A). Declinations are randomly distributed as expected due to the rotations of core segments during drilling. The distribution pattern of inclinations is also random with no distinguishable zones of higher or lower inclination, despite the 15° angle between the drilling direction and the bedding orientation. The variability in inclination can be attributed to paleosecular variation, and possibly to additional variations like the ChRM acquisition mechanism and sampling and demagnetization processes. This clearly shows that a 15° angle is not sufficient for separating normal from reversed polarity inclinations. In such cases, magnetostratigraphy must rely on the determination of the ChRM declinations by using reorientation of the core segments.

4.3. Anisotropy of magnetic susceptibility (AMS) of the WTK13 core

The results of the AMS measurements of the WTK13 core (Fig. 6, Supplementary Table III) display a significant difference in the distribution of the AMS axes between samples taken with the drill

press (Fig. 6a and b) and samples taken by pushing in a sampling cup (Fig. 6c and d). The drilled samples show mainly the typical distribution for a sedimentary fabric: the k_{\min} axes are distributed in a cone around the vertical. However, it is clear that the k_{\min} axis distribution circles around the vertical, at an angular distance of 10–20°. This is in good agreement with the angle between the core axis and sediment layers (~15°). This is consistent with the k_{\min} distribution being perpendicular to the bedding, pointing to an oblate fabric caused by compaction of the sediment, and indicating that a primarily sedimentary fabric has been preserved in these rocks (see e.g. Tarling and Hrouda, 1993). Since the core segments were not oriented, we restored the azimuthal orientation using AMS based on two possible assumptions regarding clustering of k_{\min} as will be discussed below.

The samples taken by inserting a cup into the (soft) sediment show a very typical distribution of sampling-induced AMS. The k_{\max} exhibits a clear clustering seen as a lineation, perpendicular to the pushing direction (plotted as E-W in Fig. 6c). The combined k_{\min} and k_{int} distribution shows a clear E-W girdle, which also agrees very well with the direction of compression exerted on the sediment in the cups because of pushing. Clearly, these AMS results show a classical example of a 'tectonic fabric' upon increasing compression due to sampling (Copons et al., 1997), but the results are useless for restoring orientations. These results were discarded from further interpretations. Results from 275 samples drilled from indurated sediments (Fig. 5) were not affected by sampling induced deformation of the AMS and provided a sedimentary fabric that may be used to reorient the core segment.

4.4. Re-oriented magnetostratigraphy of the WTK13 core

4.4.1. AMS-bedding reorientation

As explained in the methods section and in Fig. 7, AMS

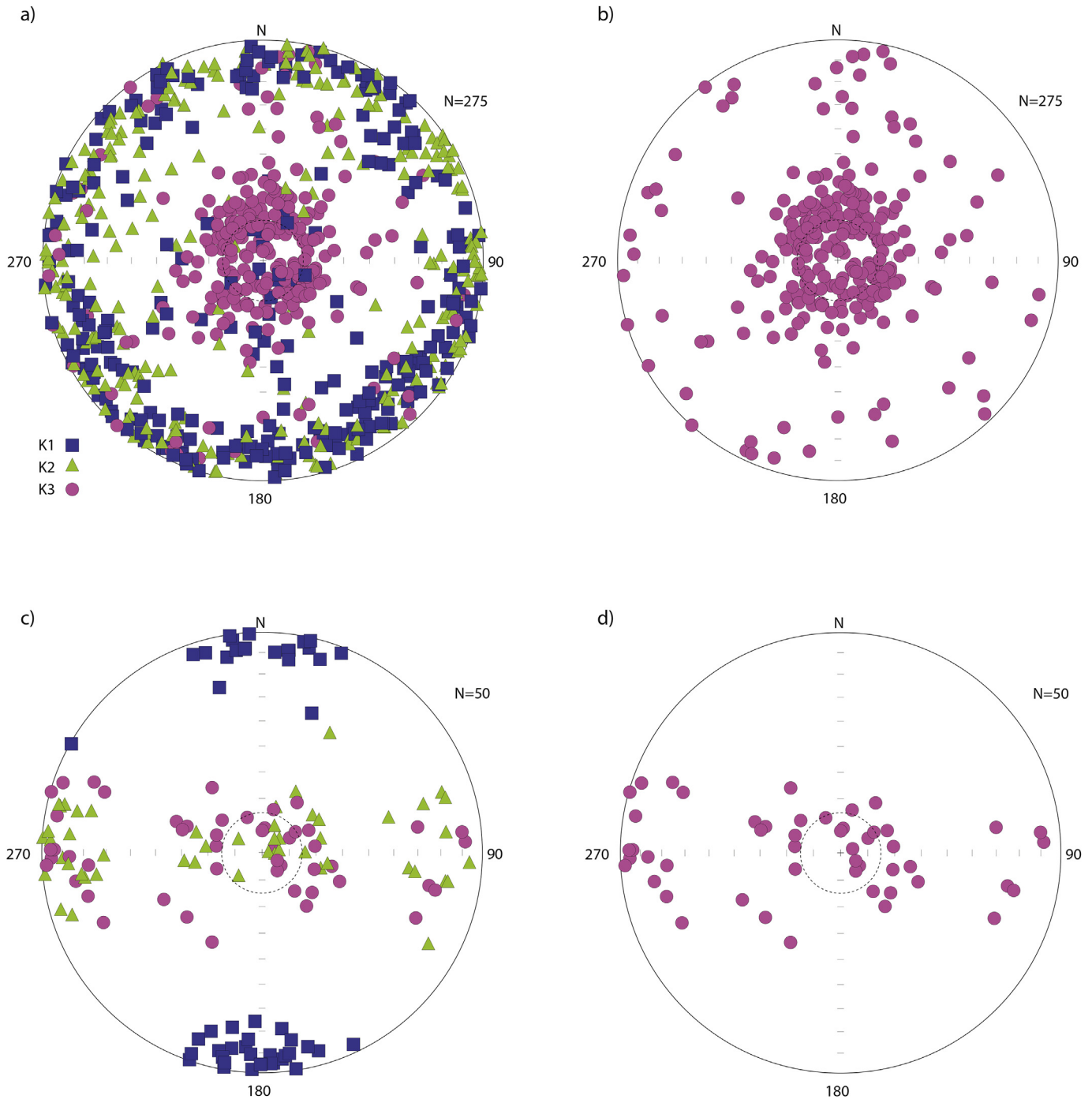


Fig. 6. a. AMS results TH samples with k1, k2 and k3 axis. b. Only k3 axis of TH samples. c. AMS results of AF samples. d. Only k3 axis of AF samples. Figure made using Anisofit42 software. Dashed circle indicates expected k3.

directions can be used to re-orientate the core segments if a sedimentary fabric is preserved with the minimum axis of the AMS tensor perpendicular to the bedding (Hrouda, 1982; Tarling and Hrouda, 1993). This method assumes the AMS as a sedimentary fabric and that the bedding of the sediments has a constant orientation throughout the core. The original AMS sedimentary fabric must not be significantly altered by tectonic or other effects such as effects induced by sampling (Copons et al., 1997). The latter is the case for the samples that were taken by pushing perspex cups into the sediment and therefore these samples are not suitable for

this method (see Fig. 6c and d).

In contrast, the AMS directions of the drilled (TH) samples appear to be suitable. From Fig. 6 it is clear that the minimum axis (k_{\min}) is largely distributed along a small circle around the vertical axis indicating an average inclination of 15° , which is indeed the expected bedding dip with respect to the core, formed by the sum of 5° bedding tilt and 10° drilling orientation. This indicates that the AMS relates to bedding and it shows that it is mostly constant throughout the core. Therefore the requirements for reorienting the core using the AMS-bedding method are met. There are a

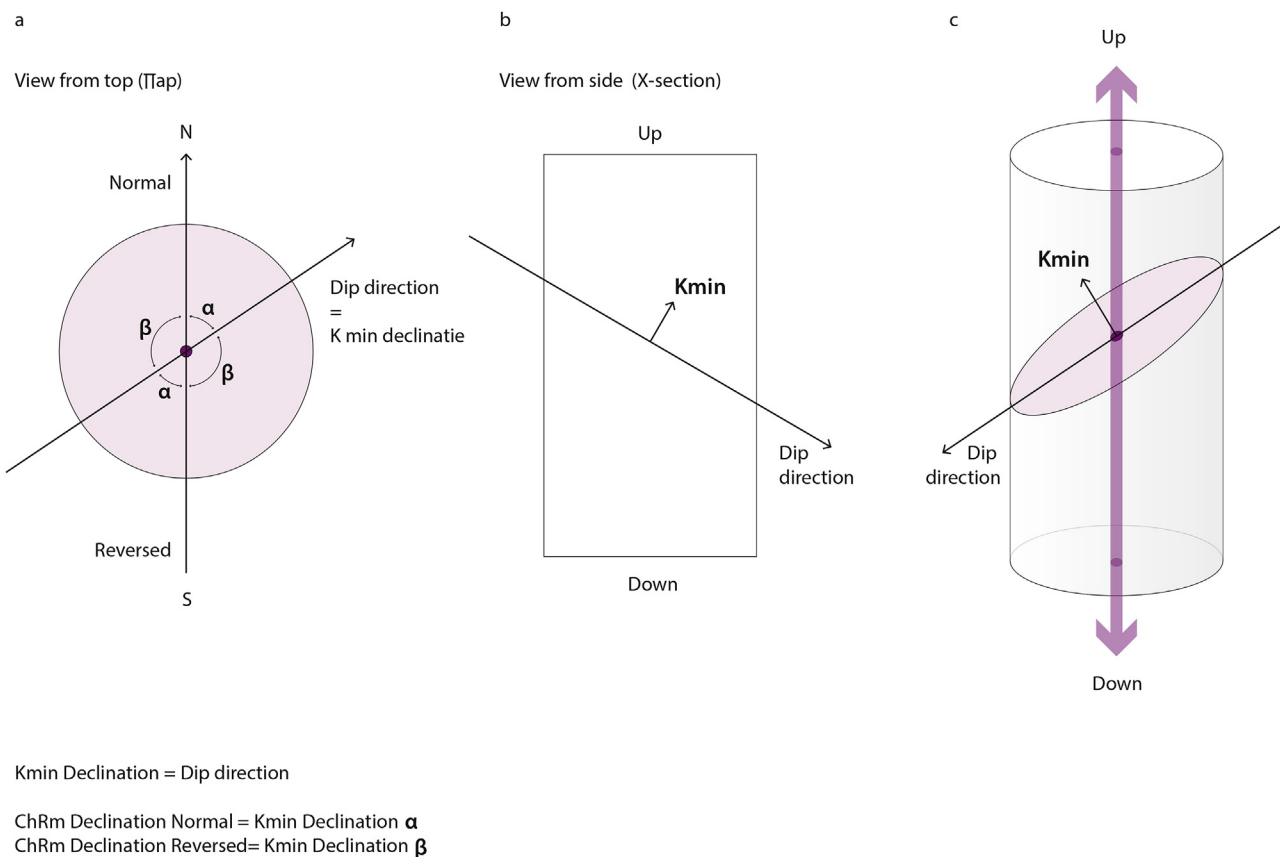


Fig. 7. AMS reorientation of WTK13 core. a. Top view. b. Side view. c. 3D view.

number of clear outliers in the k_{\min} distribution, however, which we remove based on the assumption that k_{\min} inclinations lower than $\sim 60^\circ$ are not associated with a sedimentary fabric. To do this, we ran a 45° cut-off on the VGP distribution of the k_{\min} directions, which is approximately equivalent to a 30° cut-off of the inclinations from the vertical (Supplementary Fig. 1B). By turning every ChRM direction with the amount needed to line up the k_{\min} declinations to the measured westward dip of the strata, we can place the majority of the analyzed samples in their original position (Supplementary Fig. 1C). This provides a polarity zonation with a change of normal to reversed polarity at ~ 151 mbs. Both in the upper (reversed) and lower (normal) zone there is still considerable scatter in the ChRM directions, despite the cut-off procedures on the directions (Supplementary Fig. 1C).

4.4.2. Low temperature component reorientation

To address the scatter problems mentioned above, we also used the low temperature component (LTC) that was apparent in the majority of the samples, especially if this component was anti-parallel to the high temperature component (HTC). From the anti-parallel cases we learned that the LTC was removed at $200\text{--}250^\circ\text{C}$, whereas the HTC could be determined from 200 to 250°C onward. Then, for all thermally demagnetized samples with parallel LTC and HTC, we determined the LTC and HTC using these temperature intervals (Fig. 5). Under the assumption that the LTC was a present-day overprint recorded by a small relaxation time or 'viscous' magnetic grains, we subsequently rotated the HT components – taken as the ChRM – by the angle needed to rotate the LT component to North. The rotated ChRM directions plotted against depth clearly show two polarity intervals: a lower zone with

normal polarity from -216 to -151 m and an upper zone with reversed polarity -151 to 0 m (Fig. 2). This independent method confirms the polarity determination using the AMS-bedding reorientation and yields significantly less outlying directions and no ambiguity in the polarity zonation.

5. Discussion

The magnetostratigraphy of the WTK13 core, determined using two independent reorientation methods, is straightforward with a clearly reversed zone in the upper part ($0\text{--}151$ mbs), and a clearly normal zone below 151 mbs (Fig. 2). Identifying this reversal is done by reviewing the available age constraints. The expected age range of the core is between ~ 1.4 and 1.9 Ma based on outcrop stratigraphy at the drilling site (Cohen et al., 2016; Harris et al., 1988). As part of the collaborative HSPDP work the presence of the Chari Tuff (1.38 ± 0.03 Ma) has been established near the top of the core at a level of 8 mbs (Fig. 2), based on comparative chemical fingerprinting of tuff sample 4Q-2 in the WTK13 core, and the Chari Tuff in the Kaitio outcrop (Feibel et al., 2016). The full tephrostratigraphy of the WTK13 core, including these results, will be published in detail in an upcoming separate paper within the HSPDP West Turkana collaborative framework. The presence of the Chari Tuff in the core allows us to identify the normal to reversed transition at 151 mbs as the top of the Olduvai Subchron dated to 1.778 ± 0.003 Ma (Hilgen et al., 2012). This establishes an average sediment accumulation rate of 37 cm/kyr for the upper part ($8\text{--}151.0$ mbs) of the core. Clearly, the WTK13 core does not reach the lower Olduvai Subchron boundary dated to 1.945 ± 0.04 Ma (Hilgen et al., 2012), making the bottom of the core younger than

1.945 Ma. This is consistent with the observed absence of the KBS Tuff (1.87 ± 0.02 Ma) which was not identified during the inspection and sampling of the lower parts of the WTK13 core down to 216 mbs. The absence of this tuff indicates that the sediment accumulation rates between the KBS Tuff and the top of the Olduvai Subchron must be higher than ~ 67 cm/kyr. This relatively high accumulation rate is not surprising in this particular part of the Paleolake Lorenyang sequence in the West Turkana Nachukui Formation, since it is thicker than time-equivalent sequences in the north and east of the Turkana Basin (Fig. 1D). We therefore infer that the base of the core is slightly younger than the KBS Tuff. Future work by our team will further refine this maximum age.

Another observation we can make on the basis of the WTK13 magnetostratigraphy is the absence of a reversed polarity interval in the top of the Olduvai Subchron. This putative interval would have lasted several thousands of years in a completely reversed orientation. It is very unlikely that such an event would be missed by our high-resolution sampling despite the stochastic nature of the fluvio-deltaic Turkana deposits. However, transitional intervals during a reversal and very short excursions such as the Gilsa and Gardar events may be easily missed by our record although they are reported in the sampled interval (Channell, 2017). In fact, these short excursion have never been reported in the area and are rarely observed even in the more continuous marine deposits (Channell, 2017). The observation of reversed polarities below the top of the Olduvai in the former Plio-Pleistocene global stratotype section at Vrica (Italy) led to the inferred possible existence of an additional short normal Subchron above the Olduvai, called the “Vrica Subchron” by Zijdeveld et al. (1991). The authors rejected this option, however, and placed the top of the Olduvai at the top of the Vrica Subchron. Later, Roberts et al. (2010) drilled a core at the same site as Zijdeveld et al. (1991) and identified a complex polarity pattern that they attributed to diagenetic remagnetization processes by magnetic iron sulfides. They rejected the interpretation of the reversed zone in the top of the Olduvai at the Vrica section as being a geomagnetic feature, and thus concluded that the Vrica (normal) Subchron was an artefact. However, because Roberts et al. (2010) did identify the reversed event in the top of the Olduvai in their core, the possibility of a geomagnetic event was not completely excluded. For this reason several subsequent studies have inferred the existence of a ‘Vrica event’ (referring to either a short normal zone above the top of the Olduvai Subchron, or a reversed zone within the top part of the Olduvai Subchron) in other records of the top of the Olduvai Subchron worldwide and in particular in outcrop-based studies in the Turkana region. In the Turkana Basin, Brock and Isaac (1974) identified a zone with reversed directions in the top of what they called the Olduvai Event, and mixed polarity around the Lower Illet Tuff. With the most recent age of 1.527 ± 0.014 Ma (McDougall and Brown, 2006) for the Lower Illet Tuff these directions could be the result of the paleomagnetic methods used, or the result of remagnetization of the sediments. Another possibility is that they could be related to the occurrence of the Gilsa excursion at 1.53 Ma although to this date it has not been identified in continental sediments (Channell, 2017; Singer et al., 2014). Hillhouse et al. (1977) found a complex polarity pattern in the Koobi Fora sections in Areas 102 and 103. More recent work in the Turkana Basin indicated similar polarity behavior around the upper Olduvai boundary which was interpreted as reflecting the Vrica event (Lepre et al., 2011, 2007, Lepre and Kent, 2015, 2010). However, in very high-resolution and high-quality (magnetite-bearing) sediments from the open ocean there is no trace of reversed polarities in the top of the Olduvai (e.g. Channell et al., 2016, 2003, 2002; Clement and Kent, 1987).

As shown by our rock magnetic results, the magnetomineralogy in the unweathered Turkana sediments of the WTK13 core involves

iron sulfides like pyrite and greigite, which may promote remagnetization processes during weathering of exposed outcrop sediments, and thus explain the observed complex polarity patterns in outcrop based studies. The absence of these phases in outcrops suggests that iron sulfides have been oxidized during post depositional exposure and weathering. This is further substantiated by a study of Roberts and Weaver (2005) identifying several mechanisms for the remagnetization of greigite. For example, they note the possibility of neof ormation of greigite on the surfaces of early diagenetic framboidal and nodular pyrite. Gypsum found in the outcropping deposits of alkaline East African lakes, like the Turkana Basin, could not have formed during deposition, as Ca-sulfates cannot be produced in the alkaline brine pathways that occur in these lakes (Eugster and Hardie, 1978). A more typical pathway to form gypsum has been well established, through late diagenetic/ weathering product of the oxidation of iron sulfides including pyrite (Cerling, 1979). Indeed, in the fresh core sediments we have identified the occurrence of pyrite (Feibel et al., 2016, Fig. 5a) although this has never been encountered in Lorenyang outcrop sediments (Cerling, 1979; Feibel, 1988).

Our new core-based, high-resolution, and unweathered record of the top of the Olduvai Subchron (216–151 mbs; Fig. 2) lacks any reversed event, in contrast to outcrop-based studies of the same sedimentary sequences (e.g. Lepre and Kent, 2010; Lepre et al., 2011). Based on the observed absence of any indication for reversed paleomagnetic directions we conclude that the proposed ‘Vrica event’ is most likely an artifact caused by early or late diagenetic processes.

6. Conclusions

One of the goals for the HSPDP project is to obtain high-quality fresh and unweathered sedimentary archives providing unbiased high-resolution paleoenvironmental records to be correlated to the exceptional human evolution fossil records from the area. The new paleomagnetic data from the WTK13 core provide a qualitative improvement of earlier outcrop-based magnetostratigraphic studies done in the Turkana Basin over the past decades. Our results reveal that the mineralogy carrying the remanent magnetizations preserved in the core sediments are radically different from those in previously studied outcrop sediments, with important implications for magnetostratigraphic dating. It also implies the occurrence of oxidation processes, an insight that helps to understand the observed lithologies in the outcrop and will lead to improved interpretation of depositional environments.

With the primary magnetic signal identified, our next challenge was to recover polarity orientation from the near-equatorially located WTK13 core. We developed and successfully applied two independent reorientation methods respectively, taking advantage of the preserved AMS sedimentary fabric and the occurrence of a viscous component oriented in the present day field. The reoriented directions reveal two long polarity zones separated by a polarity reversal identified as the top of the Olduvai Subchron. This provides a firm age constraint of 1.778 ± 0.003 Ma at the level of 151 mbs in the WTK13 core. The age of the top of the core is constrained by the presence of the Chari Tuff at 1.38 ± 0.03 Ma. The bottom of the core is inferred to be (slightly) younger than 1.87 ± 0.02 Ma, the age of the KBS Tuff, but further work on core-outcrop correlation is needed to establish a more precise age.

From this new magnetostratigraphic record, we find no evidence for the previously inferred Vrica Subchron. This corroborates the results of high-resolution studies of oxic (magnetite bearing) sediments with high sedimentation rates from the open ocean, which show no evidence for complex geomagnetic field behavior near the top of the Olduvai Subchron (e.g. Channell et al., 2016,

2003, 2002; Clement and Kent, 1987). We therefore conclude that late diagenetic processes most likely explain the occurrence of the apparent Vrica Subchron in outcrop records in the Turkana region, and propose that remagnetization of outcrop sediments resulted from iron sulfides that were initially present in the sediment, and were oxidized during subsequent exposure and weathering. Several recent studies have used the complex top of the Olduvai Subchron as an age constraint for dating hominin artefacts and bones, for instance Lepre et al. (2011) who described and dated the earliest Acheulian tools, and Lepre and Kent (2015, 2010) when dating the earliest *Homo erectus* skull KNM-ER 3733. Our results indicate that the complex polarity pattern near the top of the Olduvai Subchron may be a remagnetization bias which leads us to recommend caution when interpreting paleomagnetic records from outcrop sediments. If future research confirms that the Vrica Subchron is an artefact of NRM acquisition processes rather than a geomagnetic feature, this would entail age revisions for archaeological and hominin fossil occurrences that were dated based on the level assumed to define the top of the Olduvai Subchron in outcrop sediments. Hence, we caution that this apparent Vrica Subchron should not be used for paleomagnetic dating.

With the development and application of essential drill-core reorientation methods, our magnetostratigraphic record has resulted in a first age model for the WTK13 core that provides the basis for upcoming tephrostratigraphic, lithostratigraphic, paleoclimatic, and paleoenvironmental studies by the West Turkana HSPDP team.

Acknowledgements

This is publication number 10 of the Hominin Sites and Paleolakes Drilling Project. Acquisition of the HSPDP-WTK drill core and sampling was funded by the International Continental Drilling Program and US-NSF grants (EAR-1123942, BCS-1241859 and EAR-1338553). MJS, HJLvdL and JCAJ are funded by Netherlands Organisation for Scientific Research grants NWO-ALW 823.01.003, NWO-ALW 824.01.005 and NWO-ALW Veni2013 grant respectively. GDN acknowledges funding from Marie Curie CIG FP7 grant 294282 'HIRES DAT'. We thank the Kenyan National Council for Science and Technology and Kenyan Ministry of Mines for providing research and export permits, and the National Environmental Management Authority of Kenya for providing environmental permits for the drilling in West Turkana. We also like to acknowledge DOSECC Exploration Services for drilling supervision, the team of the US National Lacustrine Core Facility (LacCore) for help during drilling and sampling, the Nariokotome Mission and the people of Nariokotome, Drilling and Prospecting International Ltd, Boniface Kimeu and Francis Ekai, and the members of the West Turkana science field team: Chris Campisano, Chad Yost, Sarah Ivory, Les Dullo, Tannis McCartney, Ryan O'Grady, Gladys Tuitoek, Elizabeth Kimburi, and Thomas Johnson. Joanne Porck is thanked for her help with the figures, Carlos Saiz Domínguez for his help in the laboratory and Josep Parés for his help and advice during numerous discussions. We thank the three anonymous reviewers whose comments have greatly improved an earlier version of this manuscript.

Appendix A. Supplementary data

Supplementary data related to this article can be found at <http://dx.doi.org/10.1016/j.quageo.2017.08.004>.

References

Behrensmeyer, A.K., 2006. Climate change and human evolution. *Science* 311 (80),

- 476–478. <http://dx.doi.org/10.1126/science.1116051>.
- Brock, A., Isaac, G.L., 1974. Paleomagnetic stratigraphy and chronology of hominid-bearing sediments east of Lake Rudolf, Kenya. *Nature* 247, 344–348. <http://dx.doi.org/10.1038/247344a0>.
- Brown, F.H., Feibel, C.S., 1991. Stratigraphy, depositional environments and palaeogeography of the Koobi Fora Formation. In: Harris, J.M. (Ed.), *Koobi Fora Research Project Volume 3: Stratigraphy, Artiodactyls and Palaeoenvironments*. Clarendon Press, Oxford, pp. 1–30.
- Brown, F.H., Feibel, C.S., 1986. Revision of lithostratigraphic nomenclature in the Koobi Fora region, Kenya. *J. Geol. Soc. Lond.* 143, 297–310. <http://dx.doi.org/10.1144/gsjgs.143.2.0297>.
- Brown, F.H., Haileab, B., McDougall, I., 2006. Sequence of tuffs between the KBS tuff and the Chari tuff in the Turkana Basin, Kenya and Ethiopia. *J. Geol. Soc. Lond.* 163, 185–204. <http://dx.doi.org/10.1144/0016-764904-165>.
- Brown, F.H., McDougall, I., 2011. Geochronology of the Turkana depression of northern Kenya and southern Ethiopia. *Evol. Anthropol.* 20, 217–227. <http://dx.doi.org/10.1002/evan.20318>.
- Brown, F.H., Shuey, R.T., Croes, M.K., 1978. Magnetostratigraphy of the Shungura and Usno Formations, southwestern Ethiopia: new data and comprehensive reanalysis. *Geophys. J. Int.* 54, 519–538. <http://dx.doi.org/10.1111/j.1365-246X.1978.tb05492.x>.
- Campisano, C.J., Cohen, A.S., Arrowsmith, J.R., Asrat, A., Behrensmeyer, A.K., Brown, E.T., Deino, A.L., Deocampo, D.M., Feibel, C.S., Kingston, J.D., Lamb, H.F., Lowenstein, T.K., Noren, A., Olago, D.O., Owen, R.B., Pelletier, J.D., Potts, R., Reed, K.E., Renaut, R.W., Russell, J.M., Russell, J.L., Schabitz, F., Stone, J.R., Trauth, M.H., Wynn, J.G., 2017. The hominin sites and paleolakes drilling project: high-resolution paleoclimate records from the east African rift system and their implications for understanding the environmental context of hominin evolution. *PaleoAnthropology* 1–43.
- Cerling, T.E., 1979. Paleochemistry of plio-pleistocene Lake Turkana, Kenya. *Paleogeogr. Palaeoclimatol. Palaeoecol.* 27, 247–285. [http://dx.doi.org/10.1016/0031-0182\(79\)90105-6](http://dx.doi.org/10.1016/0031-0182(79)90105-6).
- Channell, J.E.T., 2017. Magnetic excursions in the late matuyama chron (Olduvai to matuyama-brunhes boundary) from north Atlantic IODP sites. *J. Geophys. Res. Solid Earth* 122, 773–789. <http://dx.doi.org/10.1002/2016JB013616>.
- Channell, J.E.T., Hodell, D.A., Curtis, J.H., 2016. Relative paleointensity (RPI) and oxygen isotope stratigraphy at IODP site U1308: north Atlantic RPI stack for 1.2–2.2 Ma (NARPI-2200) and age of the Olduvai Subchron. *Quat. Sci. Rev.* <http://dx.doi.org/10.1016/j.quascirev.2015.10.011>.
- Channell, J.E.T., Lubs, J., Raymo, M.E., 2003. The réunion subchronozone at ODP site 981 (Feni drift, north Atlantic). *Earth Planet. Sci. Lett.* 215, 1–12. [http://dx.doi.org/10.1016/S0012-821X\(03\)00435-7](http://dx.doi.org/10.1016/S0012-821X(03)00435-7).
- Channell, J.E.T., Mazaud, A., Sullivan, P., Turner, S., Raymo, M.E., 2002. Geomagnetic excursions and paleointensities in the matuyama chron at ocean drilling Program sites 983 and 984 (Iceland basin). *J. Geophys. Res.* 107, 2114. <http://dx.doi.org/10.1029/2001JB000491>.
- Clement, B.M., Kent, D.V., 1987. Geomagnetic polarity transition records from five hydraulic piston core sites in the north Atlantic. In: *Initial Reports of the Deep Sea Drilling Project 94*. Columbia University Academic Commons.
- Cohen, A., Campisano, C., Arrowsmith, R., Asrat, A., Behrensmeyer, A.K., Deino, A., Feibel, C., Hill, A., Johnson, R., Kingston, J., Lamb, H., Lowenstein, T., Noren, A., Olago, D., Owen, R.B., Potts, R., Reed, K., Renaut, R., Schabitz, F., Tiercelin, J.-J., Trauth, M.H., Wynn, J., Ivory, S., Brady, K., O'Grady, R., Rodysill, J., Githiiri, J., Russell, J., Foerster, V., Dommain, R., Rucina, S., Deocampo, D., Russell, J., Billingsley, A., Beck, C., Dorenbeck, G., Dullo, L., Feary, D., Garello, D., Gromig, R., Johnson, T., Junginger, A., Karanja, M., Kimburi, E., Mbuthia, A., McCartney, T., McNulty, J., Muiruri, V., Nambiro, E., Negash, E.W., Njagi, D., Wilson, J.N., Rabideaux, N., Raub, T., Sier, M.J., Smith, P., Urban, J., Warren, M., Yadeta, M., Yost, C., Zinaye, B., 2016. The Hominin Sites and Paleolakes Drilling Project: inferring the environmental context of human evolution from eastern African rift lake deposits. *Sci. Drill.* 21, 1–16. <http://dx.doi.org/10.5194/sd-21-1-2016>.
- Copons, R., Parés, J., Dinarès-Turell, J., Bordonau, J., 1997. Sampling induced AMS in soft sediments: a case study in Holocene glaciolacustrine rhythmites from Lake Barrancs (central Pyrenees, Spain). *Phys. Chem. Earth.* [http://dx.doi.org/10.1016/S0079-1946\(97\)00091-8](http://dx.doi.org/10.1016/S0079-1946(97)00091-8).
- Day, R., Fuller, M., Schmidt, V.A., 1977. Hysteresis properties of titanomagnetites: grain-size and compositional dependence. *Phys. Earth Planet. Inter.* 13, 260–267. [http://dx.doi.org/10.1016/0031-9201\(77\)90108-X](http://dx.doi.org/10.1016/0031-9201(77)90108-X).
- de Heinzelin, J., 1983. The Omo Group. Koninklijk museum voor midden-Afrika. *Geol. Wet.* 85.
- de Heinzelin, J., Haesaerts, P., 1983. The Shungura Formation. In: de Heinzelin, J. (Ed.), *The Omo Group. Koninklijk Museum Voor Midden-Afrika*, vol. 85. Geologische Wetenschappen, pp. 25–127.
- Deenen, M.H.L., Langereis, C.G., van Hinsbergen, D.J.J., Biggin, A.J., 2011. Geomagnetic secular variation and the statistics of palaeomagnetic directions. *Geophys. J. Int.* 186, 509–520. <http://dx.doi.org/10.1093/gji/ggu021>.
- deMenocal, P.B., 2011. Climate and human evolution. *Science* 80 (331), 540–542. <http://dx.doi.org/10.1126/science.1190683>.
- Dunlop, D.J., 2002b. Theory and application of the Day plot (Mrs/Ms versus Hcr/Hc) 2. Application to data for rocks, sediments, and soils. *J. Geophys. Res.* 107, 1–15.
- Dunlop, D.J.D., 2002a. Theory and application of the Day plot (Mrs/Ms versus Hcr/Hc) 1. Theoretical curves and tests using titanomagnetite data. *J. Geophys. Res.* <http://dx.doi.org/10.1029/2001JB000486>.
- Dupont-Nivet, G., Sier, M., Campisano, C.J., Arrowsmith, J.R., DiMaggio, E., Reed, K., Lockwood, C., Franke, C., Hüsing, S., 2008. Magnetostratigraphy of the eastern

- Hadar Basin (Ledi-Geraru research area, Ethiopia) and implications for hominin paleoenvironments. *Geol. Soc. Am. Spec. Pap.* 446, 67–85. [http://dx.doi.org/10.1130/2008.2446\(03\)](http://dx.doi.org/10.1130/2008.2446(03)).
- Eugster, H.P., Hardie, L.A., 1978. *Saline Lakes*. Springer New York, New York, NY. <http://dx.doi.org/10.1007/978-1-4757-1152-3>.
- Feibel, C.S., 1988. Paleoenvironments of the Koobi Fora Formation, Turkana Basin, Northern Kenya (Ph.D. thesis). The University of Utah.
- Feibel, C.S., 2011. A geological history of the Turkana Basin. *Evol. Anthropol.* 20, 206–216. <http://dx.doi.org/10.1002/evan.20331>.
- Feibel, C.S., Beck, C.C., van der Lubbe, H.J.L., Joordens, J.C.A., Sier, M.J., Beverly, M., Campisano, C., Cohen, A., 2016. The Lorenyang Lake at Kaitio: outcrop and core perspectives on an early Pleistocene lake margin. In: No. 42–46, GSA Annual Meeting Denver (Colorado).
- Feibel, C.S., Harris, J.M., Brown, F.H., 1991. Neogene paleoenvironments of the Turkana Basin. In: *Koobi Fora Research Project, Stratigraphy, Artiodactyls and Paleoenvironments*, vol. 3. Clarendon Press, Oxford, pp. 321–370.
- Feibel, C.S., Lepre, C.J., Quinn, R.L., 2009. Stratigraphy, correlation, and age estimates for fossils from Area 123, Koobi Fora. *J. Hum. Evol.* 57, 112–122. <http://dx.doi.org/10.1016/j.jhevol.2009.05.007>.
- Fisher, R., 1953. Dispersion on a sphere. *Proc. R. Soc. Lond. Ser. A. Math. Phys. Sci.* 217, 295 LP-305.
- Fuller, M., 1969. Magnetic orientation of borehole cores. *Geophysics* 34, 772–774. <http://dx.doi.org/10.1190/1.1440047>.
- Hailwood, E.A., Ding, F., 1995. Palaeomagnetic reorientation of cores and the magnetic fabric of hydrocarbon reservoir sands. *Geol. Soc. Lond. Spec. Publ.* 98, 245–258. <http://dx.doi.org/10.1144/GSL.SP.1995.098.01.15>.
- Harris, J., Leakey, R., Walker, A., 1985. Early *Homo erectus* skeleton from west Lake Turkana, Kenya. *Nature* 316, 788–792.
- Harris, J.M., Brown, F.H., Leakey, M.G., 1988. Stratigraphy and paleontology of Pliocene and Pleistocene localities west of Lake Turkana, Kenya. *Contrib. Sci.* 399, 1–128.
- Hilgen, F.J., Lourens, L.J., Van Dam, J.A., Beu, A.G., Boyes, A.F., Cooper, R.A., Krijgsman, W., Ogg, J.G., Piller, W.E., Wilson, D.S., 2012. The neogene period. In: *The Geologic Time Scale*. Elsevier, pp. 923–978. <http://dx.doi.org/10.1016/B978-0-444-59425-9.00029-9>.
- Hillhouse, J.W., Ndombi, J.W.M., Cox, A., Brock, A., 1977. Additional results on paleomagnetic stratigraphy of the Koobi Fora Formation, east of Lake Turkana (lake Rudolf), Kenya. *Nature* 265, 411–415.
- Hrouda, F., 1982. Magnetic anisotropy of rocks and its application in geology and geophysics. *Geophys. Surv.* 5, 37–82.
- Jelinek, V., 1981. Characterization of the magnetic fabric of rocks. *Tectonophysics* 79, T63–T67. [http://dx.doi.org/10.1016/0040-1951\(81\)90110-4](http://dx.doi.org/10.1016/0040-1951(81)90110-4).
- Joordens, J.C.A., Dupont-Nivet, G., Feibel, C.S., Spoor, F., Sier, M.J., van der Lubbe, J.H.J.L., Nielsen, T.K., Knul, M.V., Davies, G.R., Vonhof, H.B., 2013. Improved age control on early *Homo* fossils from the upper Burgi Member at Koobi Fora, Kenya. *J. Hum. Evol.* 65, 731–745. <http://dx.doi.org/10.1016/j.jhevol.2013.09.002>.
- Joordens, J.C.A., Vonhof, H.B., Feibel, C.S., Lourens, L.J., Dupont-Nivet, G., van der Lubbe, J.H.J.L., Sier, M.J., Davies, G.R., Kroon, D., 2011. An astronomically-tuned climate framework for hominins in the Turkana Basin. *Earth Planet. Sci. Lett.* 307, 1–8. <http://dx.doi.org/10.1016/j.epsl.2011.05.005>.
- Kidane, T., Brown, F.H., Kidney, C., 2014. Magnetostratigraphy of the fossil-rich Shungura Formation, southwest Ethiopia. *J. Afr. Earth Sci.* 97, 207–223. <http://dx.doi.org/10.1016/j.jafrearsci.2014.05.005>.
- Kidane, T., Otofui, Y.I., Brown, F.H., Takemoto, K., Eshete, G., 2007. Two normal paleomagnetic polarity intervals in the lower matuyama chron recorded in the Shungura Formation (Omo valley, southwest Ethiopia). *Earth Planet. Sci. Lett.* 262, 240–256. <http://dx.doi.org/10.1016/j.epsl.2007.07.047>.
- Kirschvink, J., 1980. The least-square line and plane and the analysis of paleomagnetic data. *Geophys. J. R. Astron. Soc.* 62, 699–718.
- Koymans, M.R., Langereis, C.G., Pastor-Galán, D., van Hinsbergen, D.J.J., 2016. Paleomagnetism.org: an online multi-platform open source environment for paleomagnetic data analysis. *Comput. Geosci.* 93. <http://dx.doi.org/10.1016/j.cageo.2016.05.007>.
- Leakey, M.G., Spoor, F., Dean, M.C., Feibel, C.S., Antón, S.C., Kiarie, C., Leakey, L.N., 2012. New fossils from Koobi Fora in northern Kenya confirm taxonomic diversity in early *Homo*. *Nature*. <http://dx.doi.org/10.1038/nature11322>.
- Lepre, C.J., Kent, D.V., 2015. Chronostratigraphy of KNM-ER 3733 and other area 104 hominins from Koobi Fora. *J. Hum. Evol.* 86, 99–111. <http://dx.doi.org/10.1016/j.jhevol.2015.06.010>.
- Lepre, C.J., Kent, D.V., 2010. New magnetostratigraphy for the Olduvai Subchron in the Koobi Fora Formation, northwest Kenya, with implications for early *Homo*. *Earth Planet. Sci. Lett.* 290, 362–374. <http://dx.doi.org/10.1016/j.epsl.2009.12.032>.
- Lepre, C.J., Quinn, R.L., Joordens, J.C.A., Swisher, C.C., Feibel, C.S., 2007. Plio-Pleistocene facies environments from the KBS Member, Koobi Fora Formation: implications for climate controls on the development of lake-margin hominin habitats in the northeast Turkana Basin (northwest Kenya). *J. Hum. Evol.* 53, 504–514. <http://dx.doi.org/10.1016/j.jhevol.2007.01.015>.
- Lepre, C.J., Roche, H., Kent, D.V., Harmand, S., Quinn, R.L., Brugal, J.-P., Texier, P.-J., Lenoble, A., Feibel, C.S., 2011. An earlier origin for the Acheulian. *Nature* 477, 82–85. <http://dx.doi.org/10.1038/nature10372>.
- Levin, N.E., 2015. Environment and climate of early human evolution. *Annu. Rev. Earth Planet. Sci.* 43, 405–429. <http://dx.doi.org/10.1146/annurev-earth-060614-105310>.
- Maddy, D., Schreve, D., Demir, T., Veldkamp, A., Wijbrans, J.R., van Gorp, W., van Hinsbergen, D.J.J., Dekkers, M.J., Scaife, R., Schoorl, J.M., Stermerdink, C., van der Schriek, T., 2015. The earliest securely-dated hominin artefact in Anatolia? *Quat. Sci. Rev.* 109, 68–75. <http://dx.doi.org/10.1016/j.quascirev.2014.11.021>.
- McDougall, I., Brown, F.H., 2008. Geochronology of the pre-KBS tuff sequence, Omo Group, Turkana Basin. *J. Geol. Soc. Lond.* 165, 549–562. <http://dx.doi.org/10.1144/0016-76492006-170>.
- McDougall, I., Brown, F.H., 2006. Precise $^{40}\text{Ar}/^{39}\text{Ar}$ geochronology for the upper Koobi Fora Formation, Turkana Basin, northern Kenya. *J. Geol. Soc. Lond.* 163, 205–220. <http://dx.doi.org/10.1144/0016-764904-166>.
- McDougall, I., Brown, F.H., Vasconcelos, P.M., Cohen, B.E., Thiede, D.S., Buchanan, M.J., 2012. New single crystal $^{40}\text{Ar}/^{39}\text{Ar}$ ages improve time scale for deposition of the Omo Group, Omo-Turkana Basin, East Africa. *J. Geol. Soc. Lond.* 169, 213–226. <http://dx.doi.org/10.1144/0016-76492010-188>.
- Mullender, T.A.T., Velzen, A.J., Dekkers, M.J., 1993. Continuous drift correction and separate identification of ferrimagnetic and paramagnetic contributions in thermomagnetic runs. *Geophys. J. Int.* 114, 663–672. <http://dx.doi.org/10.1111/j.1365-246X.1993.tb06995.x>.
- Özdemir, Ö., Dunlop, D.J., 1997. Effect of crystal defects and internal stress on the domain structure and magnetic properties of magnetite. *J. Geophys. Res.* 102, 20,211–20,224.
- Parés, J.M., Arnold, L., Duval, M., Demuro, M., Pérez-González, A., Bermúdez de Castro, J.M., Carbonell, E., Arsuaga, J.L., 2013. Reassessing the age of Atapuerca-TD6 (Spain): new paleomagnetic results. *J. Archaeol. Sci.* 40, 4586–4595. <http://dx.doi.org/10.1016/j.jas.2013.06.013>.
- Passier, H.F., Lange, G.J. De, Dekkers, M.J., 2001. Magnetic Properties and Geochemistry of the Active Oxidation Front and the Youngest Sapropel in the Eastern Mediterranean Sea, pp. 604–614.
- Peters, C., Dekkers, M.J., 2003. Selected room temperature magnetic parameters as a function of mineralogy, concentration and grain size. *Phys. Chem. Earth* 28, 659–667. [http://dx.doi.org/10.1016/S1474-7065\(03\)00120-7](http://dx.doi.org/10.1016/S1474-7065(03)00120-7).
- Potts, R., 2013. Hominin evolution in settings of strong environmental variability. *Quat. Sci. Rev.* 73, 1–13. <http://dx.doi.org/10.1016/j.quascirev.2013.04.003>.
- Roberts, A.P., Chang, L., Rowan, C.J., Horng, C.-S., Florindo, F., 2011. Magnetic properties of sedimentary greigite (Fe_3S_4): an update. *Rev. Geophys.* 49, RG1002. <http://dx.doi.org/10.1029/2010RG000336>.
- Roberts, A.P., Florindo, F., Larrasoana, J.C., O'Regan, M.A., Zhao, X., 2010. Complex polarity pattern at the former Plio-Pleistocene global stratotype section at Vrica (Italy): remagnetization by magnetic iron sulphides. *Earth Planet. Sci. Lett.* 292, 98–111. <http://dx.doi.org/10.1016/j.epsl.2010.01.025>.
- Roberts, A.P., Weaver, R., 2005. Multiple mechanisms of remagnetization involving sedimentary greigite (Fe_3S_4). *Earth Planet. Sci. Lett.* 231, 263–277. <http://dx.doi.org/10.1016/j.epsl.2004.11.024>.
- Singer, B.S., Guillou, H., Jicha, B.R., Zanella, E., Camps, P., 2014. Refining the quaternary geomagnetic instability time scale (GITS): lava flow recordings of the Blake and post-Blake excursions. *Quat. Geochronol.* 21, 16–28. <http://dx.doi.org/10.1016/j.quageo.2012.12.005>.
- Spoor, F., Gunz, P., Neubauer, S., Stelzer, S., Scott, N., Kwekason, A., Dean, M.C., 2015. Reconstructed *Homo habilis* type OH 7 suggests deep-rooted species diversity in early *Homo*. *Nature* 519, 83–86. <http://dx.doi.org/10.1038/nature14224>.
- Tarling, D.H., Hrouda, F., 1993. The magnetic anisotropy of rocks. *Tectonophysics*. [http://dx.doi.org/10.1016/0040-1951\(94\)90154-6](http://dx.doi.org/10.1016/0040-1951(94)90154-6).
- Tauxe, L., Butler, R.F., Van der Voo, R., Banerjee, S.K., 2010. *Essentials of Paleomagnetism*. University of California Press, California.
- Tauxe, L., Mullender, T., Pick, T., 1996. Potbellies, wasp-waists, and super-paramagnetism in magnetic hysteresis. *J. Geophys. Res.* 101, 571–583.
- Vasiliev, I., Dekkers, M.J., Krijgsman, W., Franke, C., Langereis, C.G., Mullender, T. a. T., 2007. Early diagenetic greigite as a recorder of the palaeomagnetic signal in Miocene-Pliocene sedimentary rocks of the Carpathian foredeep (Romania). *Geophys. J. Int.* 171, 613–629. <http://dx.doi.org/10.1111/j.1365-246X.2007.03560.x>.
- Vrba, E.S., 1995. *Paleoclimate and Evolution, with Emphasis on Human Origins*. Yale University Press, New Haven.
- Zijderveld, J.D.A., 1967. Ac demagnetization of rocks: analysis of results. *Methods palaeomagnetism*. <http://dx.doi.org/10.1016/j.neuroscience.2010.03.066>.
- Zijderveld, J.D.A., Hilgen, F.J., Langereis, C.G., Verhallen, P.J.J.M., Zachariasse, W.J., 1991. Integrated magnetostratigraphy and biostratigraphy of the upper Pliocene-lower Pleistocene from the monte singa and crotona areas in Calabria, Italy. *Earth Planet. Sci. Lett.* 107, 697–714. [http://dx.doi.org/10.1016/0012-821X\(91\)90112-U](http://dx.doi.org/10.1016/0012-821X(91)90112-U).